

Effect of polishing powder on laser damage threshold of fused silica

LIU HONGJIE^{a,*}, HUANG JIN^a, SUN LAIXI^a, LI QINGZHI^a, YE XIN^a, WANG FENGRUI^a, GENG FENG^a, JIANG XIAODONG^a, WU WEIDONG^{a,b,*}, ZHENG WANGUO^{a,b}

^aResearch Center of Laser Fusion, China Academy of Engineering Physics, Mianyang 621900, China

^bIFSA Collaborative Innovation Center, Shanghai Jiao Tong University, Shanghai 200240, China

Highly absorptive contaminants, which are introduced by polishing and buried under the optics surface, are responsible for igniting laser damage of fused silica. In order to study effects of contamination on laser-induced damage, we processed fused silica samples by using different polishing powder. We analyzed the type and relative contents of impurities on fused silica surface and tested laser damage threshold with 355nm laser irradiation. The results show that laser induced damage of the samples has obvious difference. The samples polished by Fe₂O₃ and CeO₂ have relative lower damage threshold, and the samples polished by SiO₂ and ZrO₂ have relative higher damage threshold. Microscopy images of damage morphology show that there are dense damage sites of sub-micrometer size around damage crater on the samples polished by Fe₂O₃ and CeO₂. Sub-micrometer site can not be observed by online microscopy and be regarded as damage. However, no similar damage sites of sub-micrometer size exist on other samples. This suggests that sub-micrometer damage sites have a relation with damage crater. This paper has an important significance to improve process technique of fused silica optics.

(Received August 20, 2015; accepted September 8, 2015)

Keywords: Fused silica; Laser induced damage; Contamination; Polishing powder

1. Introduction

Lifetime in the UV of fused silica optics used in large high power laser facilities such as the National Ignition Facility in the United States [1,2], the Laser MegaJoule in France [3] and the SGIII laser facility in China [4,5] has been studied extensively. The lifetime of fused silica optics is determined by both surface damage initiation and damage growth [6]. Hence, we can improve lifetime of fused silica optics through reducing initiator density and inhibiting the growth of damage sites [7]. Reports show that the intrinsic damage threshold of fused silica bulk material is higher than 100J/cm² [8, 9]. Laser-induced damage at fluence as low as a few J/cm² with nanosecond scale pulses are often attributed to subsurface defects of polished fused silica. There are two main kinds of subsurface defects: nano-metallic contaminants in the Beilby layer coming from polishing [10-12] and subsurface damage (SSD) created by grinding and/or polishing of brittle material surfaces [13, 14].

Nano-metallic contaminant has a highly absorptive character, which can ignite and induce damage. The mechanism has been researched with laser interaction experiments on gold nano-particles embedded in silica [15-17]. Papernov et al. showed that the energy absorbed by a defect of gold particle of 5 nm diameter was not enough to melt and evaporate the volume of silica to create the observed crater [15]. He also presented the damage

threshold as a function of particle size [16]. The result is that even few-nanometer-diameter particles can lead to significant threshold reduction. Kozłowski et al. detected residual impurities on chemo-mechanical polished fused silica. They found that the “gray haze” damage morphology is induced by Ce impurity [11]. Neauport et al. reported that Ce impurity has a strong influence while Al, Cu but Fe impurities have a very weak influence on damage density at 14 J/cm². And when the content of Ce impurity is low enough, the correlation between the amount of Ce and the damage density does not exist [10,12].

This paper investigates the relations between metallic impurities and laser induced damage with using the non-artificial impurity defects that are residual contamination during chemo-mechanical polishing. The types and contents of impurities are decided by polishing powder. The results show that the effect of Fe impurity on laser damage of fused silica is more severe than that of Ce impurity. The research has an important significance to improve process technique of fused silica optics.

2. Sample preparation

All fused silica samples were cutted from Corning 7980 blanks. The samples were manufactured using traditional chemo-mechanical polishing process by four kinds of polishing powder. The sample number and the

slurry type are shown in Table 1. Sample S1, S2, S3 and S4 are polished by slurry of CeO_2 , Fe_2O_3 , ZrO_2 and SiO_2 , respectively. Sample S5 is processed through rough polishing by CeO_2 and then fine polishing by ZrO_2 . Table 1 also presents surface roughness parameters measured by surface profilometer. Before damage testing, all samples were cleaned using the same cleaning procedure.

Table 1. Surface roughness of the sample with different polishing slurry

Sample	Slurry Type	Surface Roughness R_a (nm)
S1	CeO_2	0.5
S2	Fe_2O_3	0.4
S3	ZrO_2	0.5
S4	SiO_2	0.4
S5	$\text{CeO}_2+\text{ZrO}_2$	0.5

3. Metal impurities on sample surface

The types and contents of metallic impurities are tested by time-of-flight secondary ion mass spectrometry (TOF-SIMS). TOF-SIMS is capable of shallow sputter depth profiling. An ion gun is operated in the DC mode during the sputtering phase in order to remove material, and a second ion gun is operated in the pulsed mode for acquisition phase. Depth profiling by TOF-SIMS allows monitoring of all species of interest simultaneously, and with high mass resolution. The analysis area is $100 \times 100 \mu\text{m}^2$ with a spatial resolution of $1 \mu\text{m}$. All sample surfaces were sputter cleaned for ten seconds to remove contaminations induced by surroundings.

Fig. 1 shows TOF-SIMS depth profiles of subsurface on fused silica samples. By monitoring the entire mass spectrum at each depth any unexpected impurities can be detected. Sputter time represents the depth of removal material. In order to intercomparison of Samples, the relative intensity had been normalized with silicon particle number (counts 10000) as a standard. The cumulated amounts of each impurity in the fix depth are shown in Table 2. The nulls in Table 2 represent that we can not detect mass spectrum of these elements by TOF-SIMS. As shown in Fig.1 and Table 2, we can conclude that the kinds and amounts of impurities are varied for different Samples. There are many kinds of impurities (Na, Mg, Al, K, Ca, Fe and Ce etc) in the modified layer of fused silica. Nearly all Samples' surface has a lot of Al, K, Ca impurities and a small amount of B, Na, Mg impurities. Additionally, a lot of Ce impurities and a small amount of Fe impurities exist on the surface of Sample S1. A large amount of Fe impurities and a lot of Ce impurities exist on the surface of Sample S2. The surfaces of Sample S3 and S5 both have a large amount of Zr impurities, a small amount of Fe impurities and Ce impurities. The surface of Sample S4

has less kinds and amounts of impurities than other Samples.

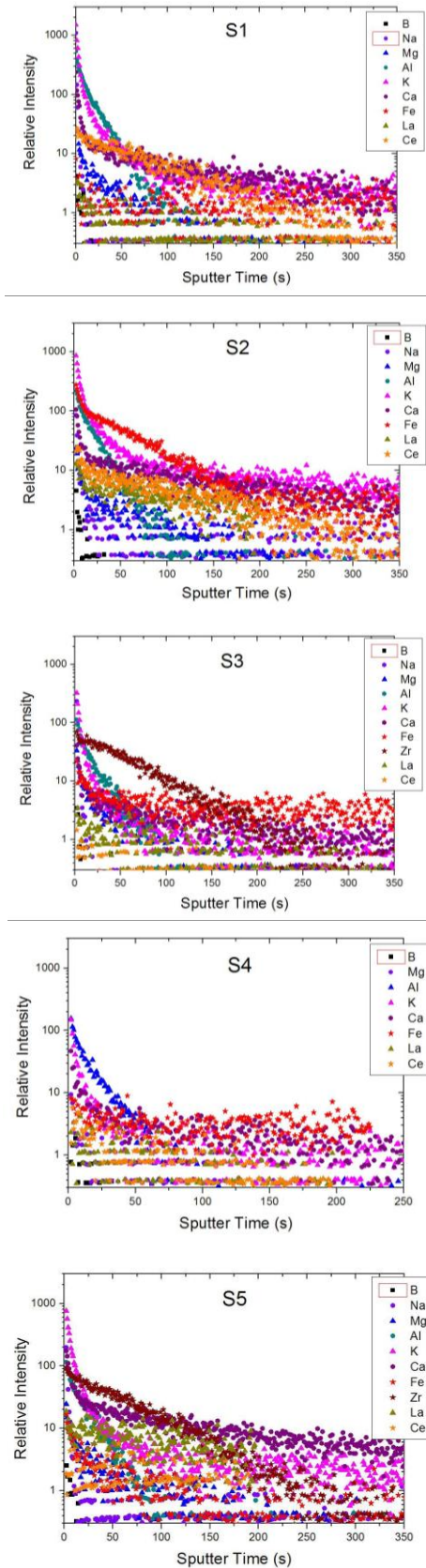


Fig. 1. Depth profiles of impurities detected on various sample subsurface

Table 2. Relative contents of metal impurities on the sample surface with different polishing slurry

Sample	B	Na	Mg	Al	K	Ca	Fe	Zr	La	Ce
S1	93	744	1636	21969	21173	8875	1130	0	481	7671
S2	98	1607	1756	13905	36913	10471	35609	0	3859	5505
S3	69	2422	2187	7117	8666	3431	4503	18219	773	159
S4	51	0	420	6828	3915	3123	3210	0	553	836
S5	75	2605	1742	7949	26439	18575	1723	23637	6072	1070

4. Laser damage performance

An experimental setup of damage performance testing system is shown in Fig. 2. Continuum laser as a seed source is a single-mode YAG laser beam with 1064nm wavelength. It is amplified through amplifier and exports 355nm wavelength with 2J maximum output energy and 9.3ns pulse duration. The output energy is adjusted by using an energy attenuator. Telescope system is applied to filter high frequency modulation and reduce the diameter of beam. An uncoated fused silica pickoff wedge reflects two beams for the diagnostic systems. A calibrated pyroelectric detector measures pulse energy proportional to the energy at the sample under test location. A beam profiler placed at the same optical distance as the sample under test location. The beam diameter size is about 3mm and the beam modulation is about 2.8 at target place. A fast photodiode allows measurement of the temporal profile. An on-line microscopy with a pixel resolution of $\sim 5\mu\text{m}$ detects rear surface damage.

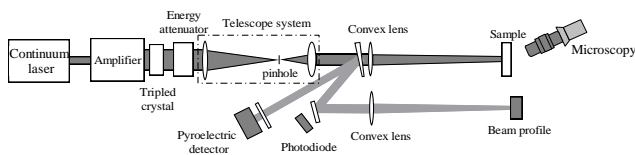


Fig. 2. Experimental setup of damage performance testing system

We measured damage threshold of sample surface by using R on 1 damage test technique [18]. The results are shown in Fig. 3, which is laser induced damage threshold on the sample surface with different polishing compounds. The damage probability curve can give information as follows: First is zero probability damage thresholds which can be considered the damage threshold of fused silica. The damage thresholds of five Samples exists apparent difference. Zero probability damage thresholds of Sample S2 ($\sim 3.2 \text{ J/cm}^2$) is far below that of Sample S4 ($\sim 7.8 \text{ J/cm}^2$). Then is the slope of damage probability curve. The

gradient of slope suggests the types of defects inducing laser damage. The more steep gradient means that 100% probability damage thresholds is nearer to zero probability damage thresholds, which suggests the less types of defects inducing laser damage.

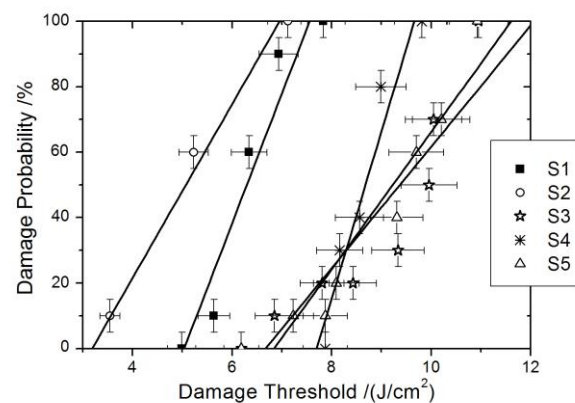


Fig. 3. Laser induced damage threshold on the sample surface with different polishing compounds

5. Analyses and discussion

We analyze the impurities and damage performance of Samples surface processed by the same technics with different polishing powder. Fig. 3 shows the sort of zero probability damage thresholds: $S2 < S1 < S3 = S5 < S4$. Impurity analyses shown in Fig. 1 and Table 2 suggest that Sample S1 has far more concentration of Fe, far less concentration of Ce and Al than Sample S2. Optical microscopy is applied to detect the morphology of ultraviolet nanosecond-pulsed-laser damage. Fig. 4 shows the morphology of laser damage on the different Samples surface. The images show that the “gray haze” damage on Sample S2 is more dense than that of Sample S1. We can conclude that Fe impurity can induce the “gray haze” damage morphology with the submicrometer size as well as Ce impurity [11]. The zero probability damage thresholds of Sample S2 ($\sim 3.2 \text{ J/cm}^2$) is lower than that of Sample S1 ($\sim 5 \text{ J/cm}^2$), so the effect of Fe impurity on the laser damage threshold of fused silica surface will not be

less than that of Ce impurity. This disagrees with previous works which believe weak or no correlations existing between damage performance of fused silica and concentration of Fe impurities [8-10,15]. Literature also reports that the correlation between amount of Ce and damage density does not exist when the content of Ce impurity is low enough [10,12]. So the differential between this paper's results and previous works may be related with the different content of Fe impurity.

The damage thresholds of Sample S3, S4 and S5 are essentially same and higher than that of Sample S1 and S2. Fig.1 and Table 2 show that a large of Zr, K, Ca impurities and a lot of La, Al impurities reside on the surface of Sample S3 and S5. This suggests that the correlations existing between damage threshold of fused silica and these impurities (Zr, K, Ca, La and Al) are weak. There are still several "gray haze" damage points in Fig. 4-S3, S4 and S5. It can be explained by the less amounts of Fe and Ce residual impurities on the surface of Sample S3, S4 and S5. The damage probability line of Sample S5 and Sample S3 is essentially coincidence. Sample S5 is first polished roughly by CeO_2 and then polished finely by ZrO_2 . This indicates that fused silica laser damage is mainly determined by the last stage of the treatment. Sample S4 has least content of impurities and highest zero probability damage threshold, which shows that SiO_2 maybe a better polishing powder.

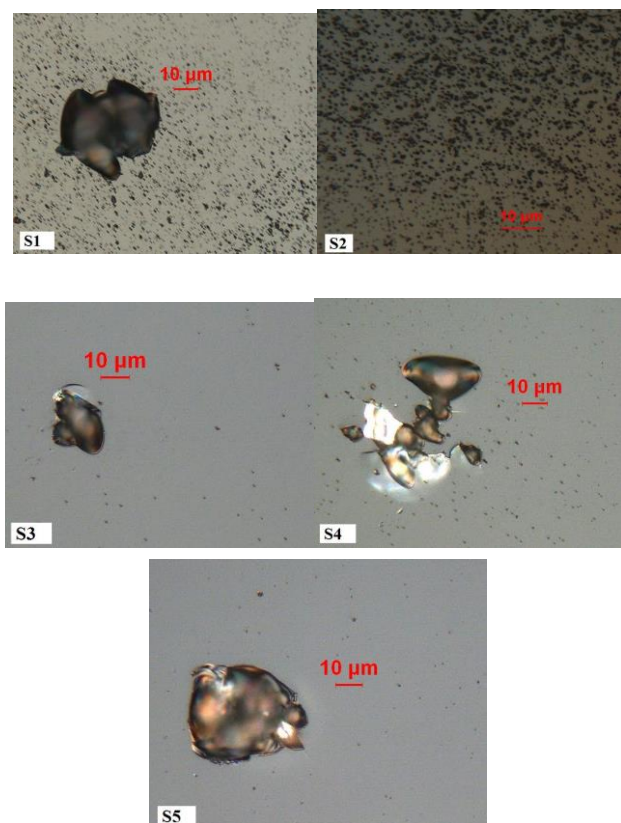


Fig. 4. Optical microscopy images of laser damage morphology. S1), S2), S3), S4) and S5) are for Sample S1, S2, S3, S4 and S5, respectively.

6. Conclusion

We have represented the impurities and damage performance of fused silica polished by different polishing powder. The results show that the sample polished by Fe_2O_3 has lowest zero probability damage threshold. It indicates that not only Ce impurity but also Fe impurity has a serious influence on laser-induced damage. The samples polished by SiO_2 and ZrO_2 have relative higher damage threshold. This suggests that the correlations existing between damage threshold of fused silica and the impurities (such as Zr, K, Ca, La and Al) are weak, and SiO_2 maybe a better polishing powder. Sample S5 shows us that fused silica laser damage is mainly determined by the last stage of the treatment. This paper is helpful to understanding laser induced damage of fused silica ignited by impurities and has an important significance to improve polishing process of fused silica optics.

Acknowledgments

The work was supported by the Development Foundation of China Academy of Engineering Physics (No.2013A0302016).

References

- [1] E. I. Moses, J. H. Campbell, C. J. Stolz, C. R. Wuest, Proc. SPIE **5001**, 1-15 (2003).
- [2] E. I. Moses, Proc. SPIE **5341**, 13 (2004).
- [3] M. L. André, in Solid state lasers for application to Inertial Confinement Fusion: Second Annual International Conference, M. L. André, ed., Proc. SPIE **3047**, 38 (1996).
- [4] H. S. Peng, X. M. Zhang, X. F. Wei, W. G. F. Jing, Z. Sui, Q. Zhao, D. Y. Fan, Z. Q. Ling, J. Q. Zhou, Proc. SPIE **4424**, 98 (2001).
- [5] G. Y. Xiao, D. Y. Fan, S. J. Wang, Z. Q. Lin, Y. Gu, J. Q. Zhu, Y. X. Zhen, J. Zhu, F. Q. Liu, S. C. Chen, Q. H. Chen, G. L. Huang, X. M. Deng, Proc. SPIE **3492**, 890 (1998).
- [6] H. Bercegol, P. Bouchut, L. Lemaignere, B. Le Garrec, G. Raze, in Proceedings of Laser-induced Damage in Optical Materials : 2003, G. J. Exarhos, A. H. Guenther, N. Kaiser, K. L. Lewis, M. J. Soileau, C. J. Stolz, Eds, Proc. SPIE **5273**, 312 (2004).
- [7] J. A. Menapace, B. Penetrante, D. Golini, A. F. Slomba, P. E. Miller, T. G. Parham, M. Nichols, J. Peterson, in Proceedings Proceedings of Laser-induced Damage in Optical Materials, G. J. Exarhos, A. H. Guenther, N. Kaiser, K. L. Lewis, M. J. Soileau, C. J. Stolz, Eds, Proc. SPIE **4679**, 56 (2001).
- [8] T. A. Laurence, J. D. Bude, S. Ly, N. Shen, M. D. Feit, Opt. Express **20**(10), 11561 (2012).

- [9] B. C. Stuart, M. D. Feit, S. Herman, A. M. Rubenchik, B. W. Shore, M. D. Perry, *Phys. Rev. B Condens. Matter* **53**(4), 1749 (1996).
- [10] J. Neauport, P. Cormont, L. Lamaignère, C. Ambard, F. Pilon, H. Bercegol, *Optics Communications* **281**, 3802 (2008).
- [11] M. R. Kozlowski, J. Carr, I. Hutcheon, R. Torres, L. Sheehan, D. Camp, M. Yan, *Proc. SPIE* **3244**, 365 (1998).
- [12] J. Neauport, L. Lamaignere, H. Bercegol, *Optics Express* **13**, 10163 (2005).
- [13] J. Neauport, P. Cormont, P. Legros, C. Ambard, J. Destribats, *Optics Express* **17**, 3543 (2009).
- [14] F. Y. Génin, A. Salleo, T. V. Pistor, L. L. Chase, *J. Opt. Soc. Am. A* **18**, 2607 (2001).
- [15] S. Papernov, A. W. Schmid, *J. Appl. Phys.* **104**, 063101 (2008).
- [16] S. Papernov, A. W. Schmid, *J. Appl. Phys.* **92**, 5720 (2002).
- [17] S. Papernov, A. W. Schmid, *J. Appl. Phys.* **97**, 114906 (2005).
- [18] J. Hue, *Proc. SPIE* **2714**, 90 (1996).

*Corresponding author: hongjie3713@163.com